INTERFEROMETRIC PHASE STACK DENOISEING VIA NONLOCAL HIGHER ORDER ROBUST PCA METHOD

Wang Rui, You Yanan, Zhou wenli

School of Information and Communication Engineering, Beijing University of Posts and Telecommunication

ABSTRACT

Interferometric stack data acquired by multi-pass synthetic aperture radar interferometry (InSAR) techniques is subject to additive outliers. Therefore, interferometric stack data denoising is an essential prerequisite for elevation inversion and terrain deformation monitoring. However, similar-patch-based denoising methods, e.g. NL-InSAR, neglect the temporal similarity between different interferograms, and tensor-based methods, e.g. Higher order Robust PCA (HoRPCA) and its evolutionary versions, can not adequately use the repeated similar fringe patterns existing in one interferogram. In our work, the limitations of NL-InSAR, HoRPCA, Weighted HoRPCA are summarized, and then a novel denoising method is proposed based on the combination of nonlocal(NL)-means and HoRPCA, named as NL-HoRPCA. This method further improves the estimation accuracy of low rank InSAR tensor. Consequently, one InSAR tensor is used to prove the superiority of NL-HoRPCA in the case of dense fringes and high outlier ratio. The accuracy results prove the robustness of the proposed method.

Index Terms— synthetic aperture radar (SAR), SAR interferometry (InSAR), tensor decomposition, NL-means, HoRPCA

1. INTRODUCTION

Interferometric stack data obtained by multi-pass synthetic aperture radar interferometry (InSAR) [1] has a wide range of applications, such as elevation inversion [2], terrain deformation monitoring [3] and so on. In fact, interferometric stack data is often corrupted by additive noise and outliers, it is difficult to be accurately decomposed to retrieve the information of topography and terrain deformation. As a result, denoising is an essential preprocessing in InSAR stack data utilization. Therefore, in this work, we mostly focus on improving denoise effect on InSAR stack data.

Many interferometric phase denoising methods has been proposed in past research, e.g., boxcar filter, Goldstein filter [4]. In recent years, nonlocal filtering and tensor filtering has gained success in InSAR data restoration. Therefore, ,interferometric stack data denoise methods proposed recenly can be divided into two categories: similar-patch-based and tensor-based method. The former one is based on the adequate fringe pattern redundancy. Theoretically speaking, this phenomenon appears because the interferometric phase is wrapped in $(-\pi, \pi]$ and similar terrain often repeats in a scope. Nonlocal InSAR (NL-InSAR) [5], as a classic denoise method, averages the center pixels of similar patches in one interferogram. Furthermore, adaptive procedure [6] are used in advanced NL-InSAR to achieve a better denoising result in complex conditions. Recently, Nonlocal Higher order Singular Value Decomposition (HoSVD) is utilized in [7] to establish the phase tensor composed of the similar patches in one interferogram, which exhibits a better performance compared to traditional nonlocal methods. However, interferograms in an InSAR stack data are time-varying. These similar-patch-based methods is limited to the appliance of spatial correlations and apparently ignore correlations between interferograms in time sequence.

The tensor-based method based on the assumption that tensor is employed as a container for InSAR stack data, and InSAR tensor presents the low-rank property. Therefore, Higher order robust principal component analyze (HoRPCA) [8], as an effective tensor decomposition method, is introduced to filter noise in the InSAR tensor as an important step to acquire accurate terrain deformation [9]. Recently, the denoise result of HoRPCA is further improved by weighting the low rank and outlier tensor, i.e. Weighted HoRPCA [10]. However, these methods do not take full advantage of the spatial similarity of repetitive fringe patterns within an interferogram, resulting in performance deterioration in some cases.

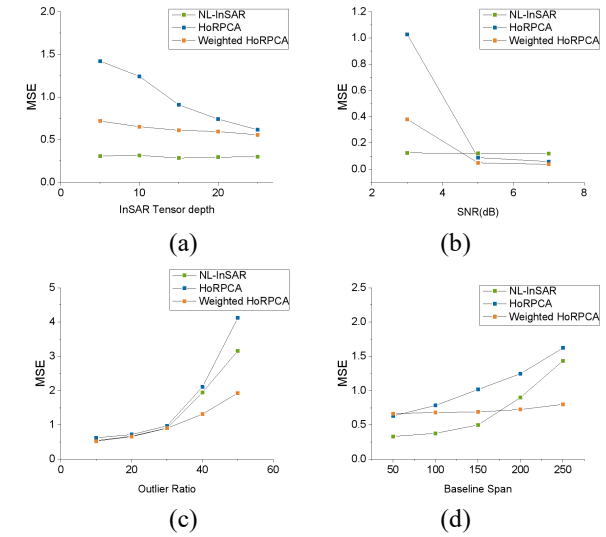

Fig. 1. Comparisons between NL-InSAR, HoRPCA and Weighted HoRPCA.

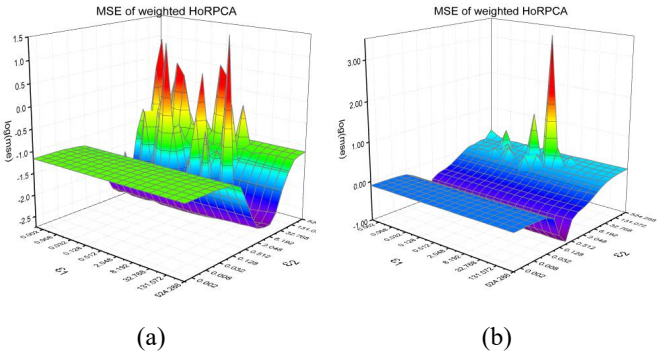

Fig. 2. MSE of Weighted HoRPCA results in parameter adjustment. (a) SNR: 5dB. (b) SNR: 10dB.

All the aforementioned methods has their own advantages. It is not easy to evaluate which approach is better in the complicated practical situation. Therefore, in this paper, we first analyze the limitations of NL-InSAR, HoRPCA, weighted HoRPCA. As a result, we try to overcome the shortcomings of the aforementioned two denoising methods and propose a novel method to filter the InSAR tensor noise, named as NL-HoRPCA.

The rest of this paper is organized as follows. Section 2 briefly introduces the limitations of InSAR denoise methods: NL-InSAR, HoRPCA and weighted HoRPCA. Section 3 presents the shortcomings of these previous methods, and then elaborates a novel NL-HoRPCA method. Section 4 has experimental results. The conclusion is given in the final part.

2. LIMITATIONS OF CLASSIC INSAR DENOISE METHOD

Generally, the NL-InSAR, HoRPCA and Weighted HoRPCA effect on InSAR stack data is mainly affected by SNR, outlier ratio and baseline span. In addition, tensor depth (the number of interferograms int the InSAR tensor) also affect the accuracy of HoRPCA and Weighted HoRPCA.

NL-InSAR is used to filter noise in one interferogram ,and the others make use of the full InSAR stack. Therefore, we average all the mean-square-error (MSE) between the noise-free and the filtered interferogram in the simulated InSAR tensor.to evaluated the result of NL-InSAR and use (1) to measure the other methods results .

$$eval = MSE(angle(result) - angle(groundtruth)) \quad (1)$$

Where $result$ is the filtered complex phase tensor and $groundtruth$ is the noise-free complex phase tensor.

As shown in Fig.1, HoRPCA requires a InSAR tensor with a relatively large number of interferograms, weak Gaussian noise, and narrow baseline span. Furthermore, the dense fringes cause more errors at the phase inconsistence in NL-InSAR. According to Fig.1, both HoRPCA and NL-InSAR are fail to hold the wide baseline span conditions.

Although Weighted HoRPCA methods can handle the problem caused by a wide baseline span, it is worthy to note that the accuracy of Weighted HoRPCA is limited by parameters initialization in weight matrix and tensor, as shown in Fig.2.

In addition, the appropriate parameters depend on SNR and other variables, so weighted HoRPCA is less stable than HoRPCA.Consequently, it is not simple to judge which method is better in the complicated practical situation. Therefore, we try to overcome the deficiency of HoRPCA and NL-InSAR.

3. NL-HORPCA

It should be noted that the utilization of spatial similarity and time similarity in the InSAR tensor is helpful for denoising. Therefore, in order to further make full use of temporal similarity, the concept of patch in NL-InSAR can be extended to 3-dimensional sub-tensor, written as $\mathcal{S}_i \in \mathbb{C}^{I_1 \times I_2 \times I_3}$, where I_1, I_2 represents the spatial dimension of a patch, I_3 represents the number of patches in interferogram series.

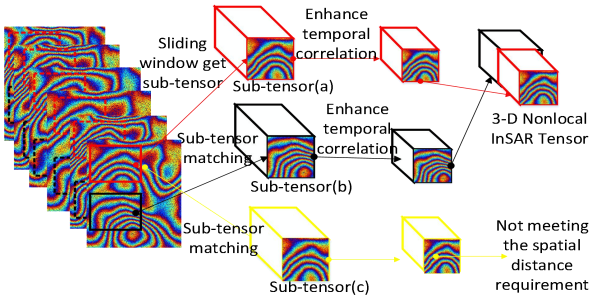

Fig. 3. The construction of NL InSAR tensor.

For each sub-tensor, a collection of similar sub-tensors can be found through the strategy shown in Fig.3. By applying the sliding window strategy, a large number of sub-tensors can be generated from a InSAR phase tensor. Then, the similarity of fringe pattern between sub-tensors is measured by Eq. (2).

$$w(\mathcal{X},\mathcal{Y}) = \left\| \mathcal{X}_{::k} - \mathcal{Y}_{::k} \right\|_{2,\alpha}^2 \tag{2}$$

where $\mathcal{X}_k$ refers to first interferogram in sub-tensor. $\left\| \cdot \right\|_{2,\alpha}^2$ is Gaussian weighted Euclidean distance. When calculating the Euclidean distance, the center pixel has a higher weight than surrounding pixels.

After calculating the similarity of sub-tensors, K-nearest neighbor algorithm is used to choose k similar sub-tensors to form a 4-dimensional tensor, named as NL InSAR tensor, written as $\mathcal{T} \in \mathbb{C}^{I_1 \times I_2 \times I_3 \times I_4}$, where I_1, I_2 represents the spatial dimension of the interferogram patches, I_3 represents the number of patches in the sub-tensor, and I_4 represents the number of similar sub-tensors. The mathematical expression of NL InSAR tensor is as follows:

$$\mathcal{T} = \left(\mathcal{S}_1 \quad \mathcal{S}_2 \quad \ldots \quad \mathcal{S}_n \right) \tag{3}$$

where $\mathcal{S}_i$ is the similar sub-tensors.

HoRPCA [8] is introduced to decompose NL InSAR tensor into low-rank and outlier tensor. Therefore, the low-rank process is modeled as follows.

$$\{\hat{\mathcal{L}}, \hat{\mathcal{E}}\} = \min_{\mathcal{L},\mathcal{E}} (Trank(\mathcal{L}) + \lambda \left\| \mathcal{E} \right\|_0), s.t. \mathcal{T} = \mathcal{L} + \mathcal{E} \tag{4}$$

where $\mathcal{T}$ is the NL InSAR tensor, $\mathcal{L}$ is the estimated low-rank tensor , $\mathcal{E}$ is the outlier tensor. $Trank(\mathcal{L})$ is the Tucker rank [11] of $\mathcal{L}$, $\left\| \mathcal{E} \right\|_0$ is the zero-norm of $\mathcal{E}$, λ is the regularization coefficient.

Since Eq. (4) is an uncertain polynomial problem, it is necessary to relax the problem by singleton model [8], which can be shown as Eq. (5).

$$\{\hat{\mathcal{L}}, \hat{\mathcal{E}}\} = \min_{\mathcal{L},\mathcal{E}} \sum_{i=1}^{3} \left\| \mathcal{L}_{(i)} \right\|_* + \lambda \left\| \mathcal{E} \right\|_1, s.t. \mathcal{T} = \mathcal{L} + \mathcal{E} \tag{5}$$

Eq. (5) can be transformed by Lagrangian multiplier algorithm into Eq. (6):

$$\min_{\mathcal{L},\mathcal{E}} \sum_{i=1}^{3} \left\| \mathcal{L}_{(i)} \right\|_* + \lambda \left\| \mathcal{E} \right\|_1 + \sum_{i=1}^{3} \left(\frac{\mu}{2} \left\| \mathcal{L}_i + \mathcal{E} - \mathcal{T} \right\|^2 - \left\langle \Lambda_i, \mathcal{L}_i + \mathcal{E} - \mathcal{T} \right\rangle \right) \tag{6}$$

where Λ_i is the Lagrangian multiplier updated literately. μ, λ is the regularization coefficient. The tensor decomposition result can be obtained by solving the Eq. (6) and using the alternating direction multiplier method (ADMM) [12].

Note that for a pixel i , several estimated value are acquired by decomposition of NL InSAR tensors, written as $\mathcal{L}_{\mathcal{T}_j}(i)$, where $\mathcal{L}_{\mathcal{T}_j}$ is low rank tensor obtained from the decomposition of $\mathcal{T}_j$ by HoRPCA, $\mathcal{T}_j$ represented j th NL InSAR tensor and its first sub-tensor contained pixel i . The final estimation of pixel i can be obtained by follows:

$$NL - HoRPCA(i) = \frac{1}{N} \sum_{j=1}^{N} \mathcal{L}_{\mathcal{T}_j}(i) \tag{6}$$

Where N is the number of NL InSAR tensors whose first sub-tensor contains pixel i .

4. EXPERIMENTAL RESULTS

In this section, the performance of NL-HoRPCA is analyzed by an InSAR tensor, containing 25 interferograms with 512 ×512 pixels for each one. This InSAR tensor is shown in Fig. 4 (a).

In order to effectively evaluate the proposed and these widespread reference methods (i.e. NL-InSAR, HoRPCA and Weighted HoRPCA), MSE between the filtered and noise-free InSAR tensor is used as an evaluation:

$$eval = MSE(angle(result) - (groundtruth)) \tag{7}$$

Since NL-InSAR is used to process interferogram instead of the whole InSAR tensor, we calculate the average of all MSEs between filtered and noise-freee interferogram in the InSAR tensor to represent the performance of NL-InSAR.

Several parts are randomly selected, and the evaluation results are shown in Table 1 and 2. As shown in Fig. 5, from the intuitive point of view, the result of NL-HoRPCA is closest to the ground truth. Table 1 illustrates that

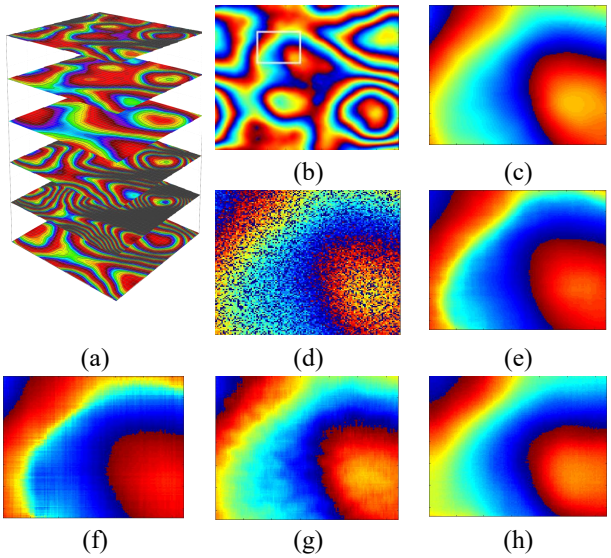

Fig. 4. The denoise results in InSAR tensor. (a) Partial InSAR tensor. (b) Ground truth. (c) Part of ground truth. (d) Partial noisy interferogram. (e) NL-InSAR. (f) HoRPCA. (g) Weighted HoRPCA. (h) NL-HoRPCA.

TABLE1 MSE on Different Baseline Span

Baseline span	NL-InSAR	HoRPCA	weighted HoRPCA	NL-HoRPCA
50	0.56	2.96	1.86	0.80
100	0.71	4.73	1.77	0.66
150	1.72	8.10	1.79	1.37
200	3.27	10.73	1.83	1.75

TABLE2 MSE on Different Outlier Ratio

Outlier	NL-InSAR	HoRPCA	weighted HoRPCA	NL-HoRPCA
20%	0.68	0.95	0.69	0.50
30%	0.85	1.46	0.94	0.75
40%	2.07	4.14	1.30	1.04

NL-HoRPCA is superior when the baseline varies widely. Table 2 proves that NL-HoRPCA has a better robustness when the ratio of outliers is increasing.

5. CONCLUSION

The interferometric phase tensor is a kind of the mathematical expression for InSAR stack data. Using the tensor as a container of the interferograms obtained by multi-pass InSAR, the decomposition of InSAR tensor can achieve the sparsity reduction and interferometric phase denoising, which is important prerequisites before extracting some geophysical parameters, such as topography, terrain deformation, and so on.

In this paper,a novel method, named as NL-HoRPCA, is proposed based on the advantages of NL-InSAR and HoRPCA. Through establishing NL InSAR tensor by using the spatial and temporal similarity. The noise of NL InSAR Tensor is eliminated with NL-HoRPCA. The experimental results prove the accuracy of this method..

6. REFERENCES

[1] A. Ferretti, C. Prati and F. Rocca, " Multibaseline InSAR DEM reconstruction: the wavelet approach," *IEEE Trans. Geosci. Remote Sens.*, vol. 37, no. 2, pp. 705–715, Mar. 1999.

[2] L. Ying, D.C. Munson, R. Koetter and B.J. Frey, " Multibaseline InSAR terrain elevation estimation: a dynamic programming approach," *Proc. Int. Conf. on Image Process.*, Sept. 14-17, 2003, pp. 157-161.

[3] P. Tantianuparp, X. G. Shi, L. Zhang, T. Balz and M. S. Liao, "Characterization of Landslide Deformations in Three Gorges Area Using Multiple InSAR Data Stacks," *Remote Sens*., vol. 5, no. 6, pp. 2704–2719, May. 2013.

[4] I. Baran, M. P. Stewart, B. M. Kampes, Z. Perski, and P. Lilly, " A modi-fication to the Goldstein radar interferogram filter, " *IEEE Trans. Geosci. Remote Sens.*, vol. 41, no. 9, pp. 2114–2118, Sep. 2003.

[5] A. Deledalle, L. Denis, and F. Tupin, "NL-InSAR: Nonlocal interferogram estimation," *IEEE Trans. Geosci. Remote Sens.,* vol. 49, no. 4, pp. 1441–1452, Apr. 2011.

[6] F. Sica, D. Reale, G. Poggi, L. Verdoliva, and G. Fornaro, " Nonlocal adaptive multilooking in sar multipass differential interferometry, " *IEEE J. Sel. Top. Appl. Earth Observ. Remote Sens.,* vol. 8, no. 4, pp. 1727-1742, Apr. 2015.

[7] X. Lin, F. Li, D. Meng, D. Hu, and C. Ding, "Nonlocal sar interferometric phase filtering through higher order singular value decompositio," *IEEE Trans. Geosci. Remote Sens. Letters,* vol. 12, no. 4, pp.806–810,Apr.2015

[8] D. Goldfarb and Z. W. Qin, "Robust low-rank tensor recovery: models and algorithms," SIAM J. Matrix Anal. Appl., vol. 35, no. 1, pp. 225–253, Nov. 2013.

[9] J. Kang, Y. Wang, M. Körner, and X. X. Zhu, " Robust object-based multipass InSAR deformation reconstruction," *IEEE Trans. Geosci. Remote Sens.*, vol. 55, no. 8, pp. 4239–4251, Aug. 2017

[10] J. Kang, Y. Wang, M. Schmitt, , and X. X. Zhu, " Object-based multipass insar via robust low-rank tensor decomposition," IEEE Trans. Geosci.Remote Sens., vol. 56, no. 6, pp. 3062–3077, Jun. 2018.

[11] L. R. Tucker, " Some mathematical notes on three-mode factor analysis," Psychometrika, vol. 31, no. 3, pp. 279–311, Aug. 1966.

[12] S. Boyd, N. Parikh, E. Chu, B. Peleato, and J. Eckstein, "Distributed optimization and statistical learning via the alternating direction method of multipliers," Found. Trends Mach. Learn., vol. 3, no. 1, pp. 1–122, Jan. 2011.